1960

A high speed dilatometric analysis of structural steels

Lawrence Frank Bubba
Lehigh University

A HIGH SPEED DILATOMETRIC ANALYSIS OF STRUCTURAL STEELS

by

Lawrence Frank Bubba

A THESIS

Presented to the Graduate Faculty

of Lehigh University

in Candidacy for the Degree of

Master of Science

Lehigh University

1960

CERTIFICATE OF APPROVAL

This thesis is accepted and approved in partial fulfillment of the requirements for the degree of Master of Science.

May 10, 1960
(Date)

H H Johnson
(Professor in Charge)

R D Stout
Head of Department of
Metallurgical Engineering

ACKNOWLEDGMENTS

The author expresses his sincere gratitude for the encouragement and guidance of Doctors Herbert H. Johnson and Robert D. Stout, Professor in Charge and Project Director respectively.

The author also extends heartfelt appreciation to the staff members of the Department of Metallurgy for their timely assistance and advice. The help of the Machine Shop staff in specimen preparation must certainly be commended.

TABLE OF CONTENTS

	Page
Acknowledgments	iii
Introduction	1
Procedure	5
Modification of Basic Dilatometer Apparatus	5
Experimental Technique	6
Metallographic and Hardness Survey	8
Discussion of Results	10
Weld Thermal Cycles	10
Analysis of Dilatometric Curves and Observed Microstructures	11
E11018 Weld Metal	11
A212 Grade B	12
A302 Grade B	13
USS T-1 and HY-80	14
AISI 4140	15
General Discussion	16
Upper Critical Temperature	16
Strain Evaluation	17
Conclusions	19
Bibliography	20
Vita	35

LIST OF TABLES

Table No.		Page
1	Chemical Analysis of the Steels Under Investigation - - - - - - - - -	21
2	Thermal and Physical Data on Selected Steels Subjected to Various Weld Thermal Cycles - - - -	22

LIST OF FIGURES

Figure No.		Page
1	Schematic Diagram of Experimental Apparatus - - - - - - - - - - - - - - -	25
2	Photomicrographs of Steels Under Investigation - - - - - - - - - - - -	26
3a	Photomicrographs of A212 - - - - - - - -	27
3b	Photomicrographs of A212 - - - - - - - -	28
4	Photomicrographs of E11018 Weld Metal	29
5	Photomicrographs of A302 - - - - - - - -	30
6a	Dilatometric Curves of A212 - - - - - -	31
6b	Dilatometric Curves of A212 - - - - - -	32
7	Dilatometric Curves of E11018 Weld Metal - - - - - - - - - - - - - - - - -	33
8	Dilatometric Curves of A302 - - - - - -	34

INTRODUCTION

Industry has long been cognizant of the fact that many of the problems arising in weldments can be attributed to microstructural changes occurring during the welding cycle. Stresses are imposed on a steel by non-uniform dimensional changes and by the transformation of austenite upon cooling. These stresses influence the weldability of the steel to an extent characteristic of the subject steel. Investigation of the transformation characteristics of various steels would enhance the understanding of their behavior during welding.

Recent investigations[1,2] substantiate the fact that certain transformation products present in the heat-affected zone of a weld exhibit a far greater susceptibility to cracking than others. A weldment is prone to cracking if a mixture of bainitic ferrite and higher carbon martensite is present. Even though both are of relatively high ultimate strength, the grain boundary material is generally of lower strength. High carbon martensite is brittle and causes the notch-toughness of the heat-affected zone to drop considerably.

The mechanical properties of hardenable steels are affected by the rapid cooling rates encountered in ordinary weld thermal cycles, and can be controlled effectively by preheating or increasing the energy input during welding. Another alternative is to use a low

carbon alloy steel whereby toughness is obtained through the formation of low carbon martensite.

A study by J. H. Gross, et al.,[3] concludes that a stress relief anneal is necessary to restore toughness to hardened areas of welded steels. Accelerated cooling refines the ferrite and carbides, thus increasing the yield and tensile strengths in heavy sections, but the toughness is sacrificed. Accelerated cooling cycles were simulated and tensile, Charpy-impact and standard end-quench tests were used to analyze the mechanical properties of heavy sections. The results were correlated with the observed microstructures.

The importance of cooling rate and the temperature of completion of austenite transformation upon cooling became increasingly evident as investigations were conducted on the weldability of specific steels. In a study of 0.5% C steel,[4] dilatation tests were used to determine the extent of transformation below an established critical temperature where cracking became prominent in the heat-affected zone. Cottrell[5] pointed out that the tendency of steel to yield hard zone cracking when welded with a given electrode can be related to the temperature of completion of austenite transformation during cooling.

As mentioned previously, internal stresses are imposed upon a steel during the welding process. Trans-formation stresses may be critical, if the steel derives

its strength from martensite, forming only in low temperature ranges of limited ductility. High strength steels of limited inherent ductility are in this category. Dilatometric techniques have proven to be particularly useful in studying the characteristic behavior of welded steels, since both thermal and transformation stresses cause dimensional changes. Investigations were conducted along these lines in the study of the weldability of C-Mn and low alloy steels.[6,7] The progress of austenite transformation during cooling has been observed with dilatometric techniques. Hardness surveys on dilatation specimens were comparable with average hardness values found in the heat-affected zone of weldability tests.

Dilatometric studies played a prominent role in determining the most suitable steel for a combination of high strength and good weldability. Critical cooling rates and transformation temperatures for hard zone cracking have been established for low carbon-low alloy steels via the aforementioned methods.

The purpose of this investigation was to study the dilatometric behavior of selected steels when subjected to weld thermal cycles. The tests cover a series of peak temperatures and cooling rates which are normally expected in welding. An effort was made to correlate the resulting microstructures, hardnesses and strains during austenite transformation upon cooling with cooling rates

and peak temperature. The problems encountered in welding, due to transformation and size-change characteristics of steels during the weld thermal cycle, have recently received wide industrial recognition. However, relatively little research has been conducted in this area.

PROCEDURE

The steels investigated were deposited weld-metal E11018, HY-80 base plate, USS T-1, A212 Grade B, A302 Grade B and AISI 4140. This selection included structural plain-carbon and high strength low-alloy steels normally used in welded structures. Table I contains the chemical analysis of the steels.

Modification of Basic Dilatometer Apparatus

The apparatus used to measure the dilation of the steel specimens was the Leitz Dilatometer, Model HTV. It was originally supplied with a resistance type furnace of 2100°F capacity for slow heating and cooling. Modification of the basic instrument included the adaption of an induction unit for fast heating and with the capacity of reaching temperatures above the melting point of the steels. The effective coupling attained between the specimen and the induction coil was the limiting factor for temperature. It became necessary to redesign the quartz vacuum tube to fit the internal diameter of the induction coil and still be adaptable to the dilatometer head. A mirror galvanometer was inserted to provide a means for recording temperature.

One other major addition to the basic dilatometer was the insertion of an external resistance to cut down

the input to the mirror galvanometer and thus increase its effective range from 2192°F (1200°C) to 2500°F (1370°C). An X-Y recorder was incorporated to provide a suitable means for determining heating and cooling rates from a time-temperature plot. Cooling rates were adjusted by the controlled introduction of helium as a quenching medium. Argon gas was used as a protective atmosphere during all heating operations.

High speed film was required to trace a dilatometric curve. Composite motion of an illuminated spot is the result of horizontal movement caused by the mirror galvanometer and vertical movement caused by specimen expansion. The rapid heating and cooling rates caused the light spot to traverse the recording end of the instrument too rapidly to allow the use of photographic paper.

Figure 1 illustrates schematically the dilatometer as modified and used during this investigation.

Experimental Technique

Nine specimens approximately 50 mm long and 3.2 mm in diameter were machined from each of the steels surveyed, the exact length before and after heating being recorded in Table II. Each specimen was placed in position in the quartz tube and a 28 gauge chromel-alumel thermocouple was spark welded to the center of the specimen. Spark welding insured good contact and eliminated a bead which might

have been affected by the induction heating. The thermocouple leads fed the mirror galvanometer and a Speedomax "H" temperature indicator, each calibrated for 2500°F by use of an external resistance. The thermocouple was hooked directly to an X-Y recorder which was provided with a discharge capacitor to produce a time axis for heating and cooling rate curves.

With the induction coil in place the specimen was heated in an argon atmosphere, in all cases, to the Ac_1 in an interval of 5 seconds. When transformation was detected by observing a drop in amperage, due to reaching the Curie temperature, full power was applied until the peak temperature was attained. At this point the power input was cut off and the specimen was quenched with helium. When room temperature was reached, the film was removed from the dilatometer and developed.

Each steel was subjected to nine thermal cycles as depicted below:

Approximate Peak Temperature, °F	Average Time to Peak Temperature	Approximate Cooling Rates at 1300°F, °F/sec.
1625°F	8.6 sec.	135, 60, 30
2035°F	17.8 sec.	135, 60, 30
2375°F	18.3 sec.	135, 60, 30

Considerable difficulty was realized in controlling cooling rates by regulating the helium flow. The actual cooling rate at 1300°F was calculated from the time-temperature

curves and was recorded in Table II.

The dilatometric curves were analyzed for transformation temperatures, and the transformation and residual strains were calculated by dividing the change in length by the initial length at the respective temperatures.

Metallographic and Hardness Survey

Metallographic specimens were prepared for each steel in the as-received condition, Figure 2, and after subjection to each thermal cycle. Vickers pyramid hardness readings were taken and recorded with the composite data in Table II. Photomicrographs were taken for A212, A302 and weld-metal subjected to the thermal cycles as listed below:

Material	Peak Temp.	Cooling Rate at 1300°F
A212	1635°F	168 °F/sec.
	1610°F	34.7 °F/sec.
	2390°F	131.3 °F/sec.
	2425°F	21.7 °F/sec.
A302	2035°F	118 °F/sec.
	2080°F	24.3 °F/sec.
[illegible]	2370°F	136.7 °F/sec.
	2385°F	25.3 °F/sec.

The resultant microstructures are presented in Figures 3A through 5. The dilatometric curves for each of these runs are presented in Figures 6 through 9. The micro-

structures for each steel under every thermal cycle were examined and correlated with existent conditions.

DISCUSSION OF RESULTS

Weld Thermal Cycles

The choice of peak temperatures and cooling rates selected for this investigation were believed to be fairly representative of the thermal cycles encountered at various positions in a weld. Not included in this phase of the work was the variation which can be expected in heating rates at various positions in a weld. The data clearly illustrate the difficulty encountered in reproducing a specific cooling rate for each steel at a certain peak temperature. The cooling rates vary from 180°F/sec. to 112.5°F/sec. for the fast cooling, 82°F/sec. to 45.8°F/sec. for the intermediate cooling, and 42.8°F/sec. to 19.2°F/sec. for the slow cooling. These rates average out to 135°F/sec., 57.3°F/sec., and 28.8°F/sec., respectively. Intended values were 130°F/sec., 60°F/sec., and 30°F/sec.

Temperatures varied from 1605°F to 2400°F with the averages 1625°F, 2035°F, and 2375°F being fairly close to the intended value. The primary objective was to achieve peak temperatures as rapidly as possible without excessive distortion of the dilatometric curve.

Analysis of the Dilatometric Curves and Observed Microstructures

E11018 Weld Metal

Specimens of E11018 weld metal were prepared from the center of a multiple pass weld which meant that the material had already undergone the effects of several weld thermal cycles. This accounted for the relatively minor change in microstructure of the specimens from the as received structure, chiefly bainite and ferrite.

The relatively short times at peak temperature did not permit complete austenitization close to the Ac_3. Homogenization increased, however, as the temperatures were raised. The basic microstructure was bainite and ferrite with increasing mounts of the latter as the cooling rates were reduced. The low carbon content of the material practically eliminated the possibility of martensite forming, even with the rapid cooling rate from high peak temperatures.

From the dilatometric curves it was observed that at the intermediate and slow cooling rates, respectively, the transformation range of temperatures was relatively the same at all peak temperatures. This correlated with the observed microstructures. At the fast cooling rates the highest peak temperature produced predominantly banitic structures, with a slight possibility of some low carbon

martensite. Examination of the hardness data supported the microstructure observations.

Transformation and residual strains were calculated by measuring the dilation at transformation and the overall expansion or contraction, and dividing these measurements by the original lengths respectively. The transformation strain generally increased with decrease in cooling rate and with increasing amounts of higher temperature transformation products. The residual strain averaged out to .0497% and generally increased with increase in peak temperature. The significance of the strain values is discussed later.

A212 - Grade B

Specimens were prepared from A212 - Grade B steel in the as-rolled condition. The microstructure was lamellar pearlite and blocky ferrite. As the material was subjected to the low peak temperature, the pearlite became more refined with an increase in cooling rate. Again the relatively short time at temperature and the rapid heating rate undoubtedly left some ferrite untransformed, and upon rapid cooling yielded the structure shown in Figure 2A, austenite transformed to fine pearlite and was surrounded by blocky ferrite.

The intermediate and nigh peak temperatures at fast cooling rates produced some hardening. The predominant

structures, however, were fine pearlite with increasing amounts of acicular ferrite as the cooling rate was decreased. Once again the hardness survey corroborated the microstructural observations.

Analysis of the dilatometric curves showed that increasing the peak temperature lowered the transformation temperature for the respective cooling rates. These transformation temperatures when correlated with isothermal transformation diagrams for plain carbon steel[8] further support the microstructure observations.

A212 exhibited a very low average residual strain, 0.0077%, with slight over-all contraction only at the high peak temperature. The transformation strain generally decreased with decrease in cooling rate for the low and intermediate peak temperatures. At the high peak temperature the pattern was irregular.

A302 - Grade B

This steel was received in a normalized condition with an initial structure of ferrite and slightly spherodized carbides. As was expected, the high manganese content with the molybdenum added produced hardening in all cases. The low peak temperature produced some martensite on fast cooling, and increasing amounts of fine-grained ferrite and pearlite as the cooling rate was reduced. At the intermediate peak temperature all martensite was produced

on fast cooling and essentially all bainite on slow cooling, these structures being presented in Figure 3. As the cooling rate was reduced, the structure progressed from martensite to martensite with increasing amounts of banite for the high peak temperature.

The dilatometric curves were in keeping with the observations already discussed. A302 exhibited transformation temperatures lower than those of E11018 and A212 for relatively the same thermal cycles. This was expected because of the higher hardenability. Formation of lower temperature transformation products was substantiated through comparison of the hardness surveys for each steel.

An average residual strain of 0.0604% was calculated for A302. The transformation strain was irregular at the low peak temperature but showed a general tendency to decrease with cooling rate during the other thermal cycles.

USS T-1 and HY-80

Each of these steels was received in the quenched and tempered condition. Their behavior was much the same during each thermal cycle with martensite forming upon fast cooling from all peak temperatures. At the low peak temperature the slow and intermediate cooling rates yielded essentially all bainite. There were

mixtures of bainite and martensite with increasing amounts of acicular bainite at slower cooling rates from the intermediate and high peak temperatures.

One interesting point uncovered upon analysis of the dilatometric curves was the relatively short temperature range covered by T-1 during transformation. There was an overlapping of transformation temperature ranges for both materials as might be expected from the microstrucutral studies. Comparison of hardness surveys did not reveal any general trend except fairly good agreement between both steels at low and high peak temperatures. The intermediate peak temperature hardness values indicate the HY-80 possibly contains more martensite of slightly higher carbon content. This was insufficient basis, however, to form a generalization.

T-1 displayed a higher average residual strain than HY-80, 0.0679% and 0.0552% respectively. The transformation strain of T-1 decreased with cooling rate for low and high peak temperatures but increased at the intermediate peak temperature. It, however, was generally higher than the transformation strains of HY-80, which decreased with cooling rate during all thermal cycles.

AISI 4140

The AISI 4140 was the highest carbon steel investigated. It was used in the as-rolled condition and initially

appeared to be bainite and ferrite with some pearlite. This structure transformed to martensite at all peak temperatures and cooling rates except the slow cools. Here there were structures ranging from complete bainite to bainite with an estimated 10%-15% martensite. The high carbon martensite was found to be the hardest structure observed.

Information obtained from the dilatometric curves showed the material transforming at a range of temperatures lower than that for the other steels investigated. The high carbon content lowers the M_s temperature, thus explaining the high hardenability.

One unique observation made was that AISI 4140 had an over-all expansion for the fast and intermediate cools at low and medium peak temperatures. This made the residual strain average out to 0.0120%. The transformation strain was lowered with cooling rate for the low and intermediate peak temperature cycles, but it was observed to increase at the high peak temperature.

General Discussion

Upper Critical Temperature

No mention has been made concerning the transformation on heating. The range of temperatures covered was from 1292°F for A302 to 1343°F for USS T-1, manganese being chiefly responsible of the lower upper critical of A302. The plain carbon A212 and the A302 steels experienced

less dilation during transformation on heating than the other steels. Comparison of Figures 6a and 8 with Figure 7 illustrates this. The temperatures of transformation on heating are fairly consistent for the respective steels. Slight variations were encountered due to small differences in heating rate and film evaluation.

Strain Evaluation

The significance of the transformation strains and residual strains was not fully appreciated until approximate stress calculations were made. For illustrative purposes, the maximum and minimum observed transformation strains were used. These were USS T-1, heated to a peak of 2010°F and cooled at 59.7°F/sec., and A212, heated to a peak of 2390°F and cooled at 131.3°F/sec., respectively. The T-1 (low-alloy) transformed on cooling between 770°F-710°F, and the A212 (plain carbon) transformed between 955°F-860°F. The transformation products were martensite with some bainite for USS T-1 and refined pearlite with acicular ferrite and very little martensite for A212.

Hooke's law of stress equal strain times the Modulus of Elasticity was employed. A thermal coefficient for the Modulus of Elasticity was used to compensate for the temperature.[9] For USS T-1 the transformation stress was .00427 x 0.861 x 30 x 10^6 or 110,294 psi, and for A212

it was .00108 x 0.825 x 30 x 10^6 or 25,730 psi. At 750°F the yield strength for USS T-1 is 98,300 psi,[10] therefore it was concluded that the transformation stress was sufficient to cause plastic flow. Only then did the true significance of the measured strain values become evident.

The general trend was that the alloy steels had greater transformation and residual stresses than the other steels investigated. The plain carbon steel had the least residual and transformation stresses measured.

CONCLUSIONS

The results of the investigation may be summarized as follows:

1. Microstructural observations were corroborated by information collected from analysis of the dilatometric curves and were in general agreement with expectations derived from isothermal transformation diagrams.
2. There was more consistency in the results of the plain carbon steel and weld metal than in the low alloy steels. The plain carbon steel exhibited a much lower residual stress than any other steel investigated, and it had a lower transformation stress than any of the low alloy steels.
3. In the alloy steels the residual and transformation stress increase as the alloy content increases. The transformation temperatures on cooling decrease with alloy and carbon content, and the shape of the dilatometric curves are affected markedly by alloy content.
4. Careful analysis of dilatometric curves provide much useful information concerning transformation characteristics of the material under investigation. With some modifications to permit stringent control over the thermal cycles and to insure more precise measurement and evaluation of the curves, the dilatometric analysis can become an indispensable tool in the study of transformation characteristics of materials.

BIBLIOGRAPHY

1. J. T. Berry and R. C. Allan, "Cracking in Low Alloy Steel Welded Joints", Welding Journal, 39 (3), (March, 1960) pp. 105s-115s.

2. E. F. Nippes, "The Weld Heat-Affected Zone," ibid., 38 (1), (January, 1959) pp. 1s-19s.

3. J. H. Gross, E. H. Kottcamp and R. D. Stout, "Effect of Heat-Treatment on the Microstructure and Low Temperature Properties of Pressure-Vessel Steels," ibid., 37 (4), (April, 1958) pp. 160s-169s.

4. B. J. Bradstreet and R. L. Wilkins," Continuous Cooling Transformation Characteristics Related to Weldability of 0.5% C Steel," British Welding Journal, 2 (12), (December, 1955) pp. 562-566.

5. C. L. M. Cottrell, "Weldability of Mn-Mo Steel Related to Properties of the Heat-Affected Zone," ibid., 1 (4), (April, 1954) pp. 177-187.

6. C. L. M. Cottrell, B. J. Bradstreet and T. E. M. Jones, "Weldability and Mechanical Properties of a Series of Mn-Ni-Cr-Mo Steels," ibid., 3 (3), (March, 1956) pp. 90-98.

7. C. L. M. Cottrell, "Weldability of C-Mn Steel Related to Properties of Heat-Affected Zone," ibid., 2 (2), (February, 1955) pp. 75-80.

8. U. S. Steel Corp., "Atlas of Isothermal Transformation Diagrams," (1951).

9. D. K. Bullens, "Steel and Its Heat-Treatment," vol. III, 5th edition, pp. 361.

10. J. H. Gross and R. D. Stout, "The Performance of High-Strength Pressure Vessel Steels," Welding Journal, 21 (3), (March, 1956) pp. 115s-120s.

TABLE I

CHEMICAL ANALYSIS STEELS INVESTIGATED

Steel	Composition										
	C	Mn	P	S	Si	Ni	Cr	Mo	Cu	V	B
A212 Grade B	0.28	0.70	0.010	0.021	0.24						
A302 Grade B	0.20	1.32	0.022	0.030	0.25			0.42			
USS T-1	0.15	0.93	0.015	0.022	0.27	0.89	0.48	0.44		0.06	0.0031
AISI 4140	0.39	0.76	0.015	0.019	0.23		0.94	0.18			
HY-80	0.16	0.31	0.016	0.0305	0.20	2.86	1.37	0.21	0.18		
E11018											

TABLE II

THERMAL AND PHYSICAL DATA ON SELECTED STEELS SUBJECTED TO VARIOUS THERMAL CYCLES

Steel	Peak Temp. °F	Cooling Rate at 1300°F °F/sec	Transf. Temp. on Heating °F	Transf. Temp. on Cooling, °F, Start-End: Horizontal Tangency Pts.	Transf. Temp. on Cooling, °F, Start-End: Change of Slope Pts.	Original Length mm	Final Length mm	Transf. Strain %	Residual Strain %	Original Hardness VPN	Final Hardness VPN
E11018	1630	126	1325	935 - 800	980 - 680	49.91	49.89	.130	.0401	287	281
Weld-	1685	49.5	1300	1010 - 880	1065 - 825	50.24	50.23	.218	.0199		262
Metal	1650	32.6	1325	1035 - 885	1100 - 850	49.84	49.81	.220	.0502		240
	2045	130	1325	915 - 780	965 - 735	50.50	50.46	.128	.0792		297
	2025	45.8	1315	985 - 875	1040 - 800	50.06	50.04	.249	.0400		262
	2050	26.7	1325	1005 - 875	1040 - 775	49.91	49.89	.260	.0301		235
	2370	136.7	1320	800 - 590	850 - 550	50.62	50.60	.206	.0396		322
	2380	56.5	1315	960 - 840	1040 - 780	50.29	50.25	.208	.0796		282
	2385	25.3	1315	980 - 860	1055 - 790	50.51	50.51	.257	.0594		246
A212	1635	168	1310	1130 - 1035	1155 -1030	50.32	50.32	.158	0	168	195
Grade	1625	48.2	1290	1175 - 1070	1210 -1070	50.67	50.67	.157	0		183
B	1610	34.7	1300	1260 - 1120	1315 -1120	50.53	50.53	.147	0		179
	2060	180	1300	940 - 930	965 - 920	50.64	50.64	.314	0		209
	2020	56.6	1300	1140 - 1100	1180 -1100	50.57	50.57	.265	0		196
	2050	30.9	1310	1175 - 1130	1230 -1130	50.57	50.57	.236	0		181
	2390	131.3	1320	955 - 860	980 - 840	50.85	50.83	.108	.0295		258
	2385	46.8	1305	1100 - 1080	1165 -1080	50.60	50.59	.266	.0198		203
	2425	21.7	1315	1155 - 1130	1180 -1130	50.34	50.33	.267	.0199		197

TABLE II (cont'd)
THERMAL AND PHYSICAL DATA ON SELECTED STEELS
SUBJECTED TO VARIOUS THERMAL CYCLES

Steel	Peak Temp. °F	Cooling Rate at 1300°F °F/sec.	Transf. Temp. on Heating °F	Transf. Temp. on Cooling, °F, Start-End: Horizontal Tangency Pts.	Transf. Temp. on Cooling, °F, Start-End: Change of Slope Pts.	Original Length mm	Final Length mm	Transf. Strain %	Residual Strain %	Original Hardness VPN	Final Hardness VPN
A302	1610	168	1300	715 - 625	650 - 485	50.64	50.62	.128	.0396	187	369
Grade	1610	62.7	1290	960 - 860	975 - 835	50.83	50.78	.127	.0886		300
B	1605	36	1280	985 - 880	1015 - 840	50.36	50.30	.158	.1190		266
	2035	118	1320	675 - 560	685 - 525	50.66	50.65	.336	.0194		437
	2050	55	1270	865 - 760	915 - 680	50.61	50.60	.296	.0195		341
	2080	24.3	1280	940 - 850	1000 - 800	50.65	50.62	.266	.0593		271
	2330	122.8	1290	640 - 535	655 - 520	50.64	50.61	.366	.0692		427
	2370	54.6	1305	860 - 770	900 - 725	50.43	50.40	.288	.0591		333
	2370	30.4	1315	915 - 840	935 - 800	50.71	50.67	.305	.0696		267
USS	1635	163	1355	660 - 590	675 - 575	50.80	50.77	.325	.0552	297	375
T-1	1610	76.2	1340	770 - 690	800 - 670	50.08	50.06	.300	.0500		357
	1630	32.9	1350	870 - 785	915 - 710	50.11	50.08	.249	.0599		302
	1985	166	1350	720 - 610	740 - 575	50.46	50.42	.308	.0792		390
	2010	59.7	1330	770 - 710	790 - 680	50.52	50.48	.416	.0791		379
	2035	32.3	1340	805 - 780	815 - 720	50.31	50.27	.427	.0794		327
	2400	121.7	1350	700 - 575	700 - 550	51.21	51.17	.333	.0797		419
	2350	54.3	1350	775 - 705	825 - 630	50.51	50.48	.366	.0496		410
	2365	19.2	1345	860 - 800	875 - 740	50.64	50.60	.376	.0791		312

TABLE II (cont'd)

THERMAL AND PHYSICAL DATA ON SELECTED STEELS

SUBJECTED TO VARIOUS THERMAL CYCLES

Steel	Peak Temp. °F	Cooling Rate at 1300°F °F/sec.	Transf. Temp. on Heating °F	Transf. Temp. on Cooling, °F, Start-End		Original Length mm	Final Length mm	Transf. Strain %	Residual Strain %	Original Hardness VPN	Final Hardness VPN
				Horizontal Tangency Pts.	Change of Slope Pts.						
HY-80	1650	127.7	1335	750 - 615	780 - 600	50.28	50.24	.169	.0894	221	339
	1625	66	1325	840 - 680	865 - 665	50.19	50.14	.149	.0994		322
	1610	24.6	1290	875 - 725	900 - 715	50.27	50.19	.129	.1690		295
	2050	170.5	1325	565 - 480	575 - 465	50.52	50.51	.376	.0198		405
	2010	48.2	1350	860 - 680	880 - 650	50.53	50.52	.227	.0099		390
	2030	31.5	1340	865 - 720	900 - 660	50.58	50.57	.217	.0198		317
	2360	158	1335	665 - 500	670 - 475	50.64	50.62	.326	.0395		408
	2400	54.2	1340	745 - 610	785 - 585	50.53	50.51	.357	.0396		383
	2375	23.3	1350	870 - 780	885 - 710	50.44	50.42	.307	.0397		310
A1S1	1605	112.5	1310	600 - 470	630 - 450	50.36	50.38	.158	.0298*	292	383
4140	1610	82	1290	540 - 425	600 - 400	50.20	50.20	.157	0		339
	1610	42.8	1320	885 - 775	915 - 750	51.31	51.27	.147	.0682		369
	2015	138	1310	575 - 445	600 - 430	50.38	50.41	.314	.0595*		548
	2020	61.1	1290	575 - 415	615 - 385	50.60	50.61	.265	.0195*		503
	2060	26.9	1310	865 - 815	885 - 800	50.50	50.48	.236	.0297		339
	2350	126	1310	560 - 410	575 - 390	50.29	50.28	.108	.0099		536
	2370	54.2	1315	630 - 450	720 - 415	50.37	50.34	.266	.0596		536
	2360	24.2	1315	850 - 815	875 - 780	50.50	50.48	.267	.0495		322

* Expansion

Figure 1. Schematic Diagram of Experimental Apparatus.

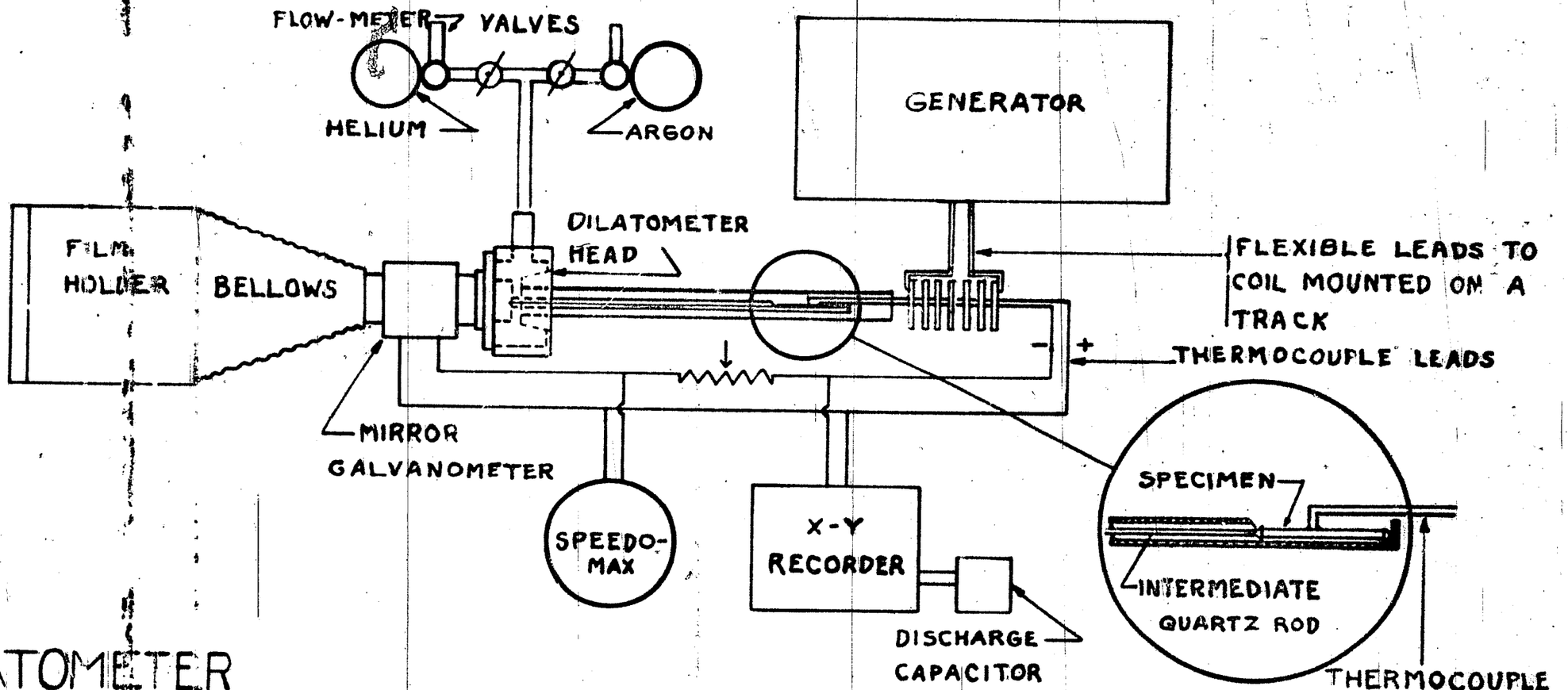

DILATOMETER

Figure 2. Photomicrographs of Steels Under Investigation.

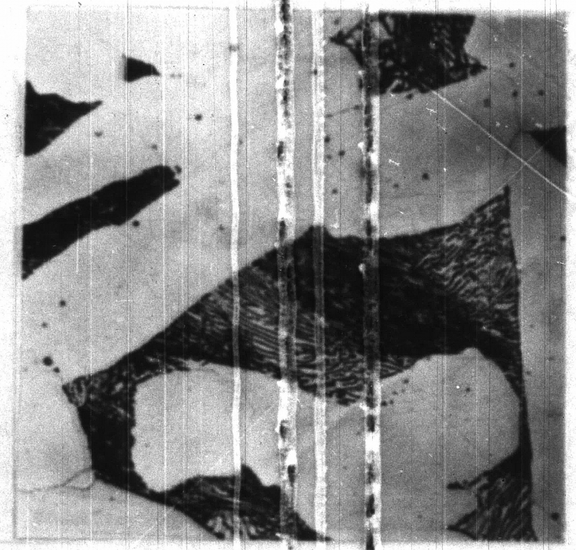

A-212 As Rolled VPN 168
1000 X Nital-Picral

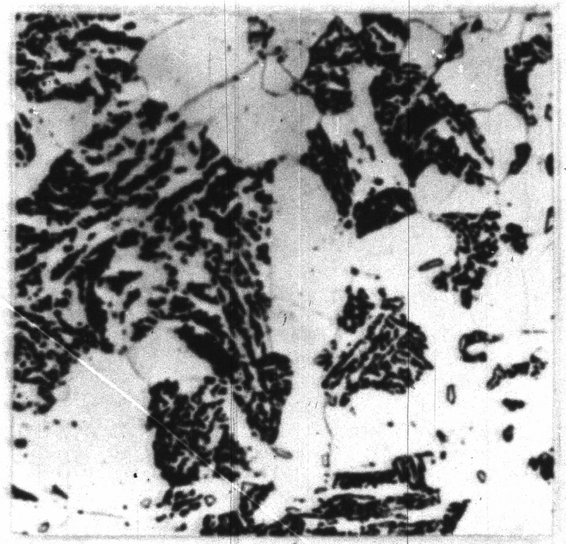

A-302 Normalized VPN 187
1000 X Nital-Picral

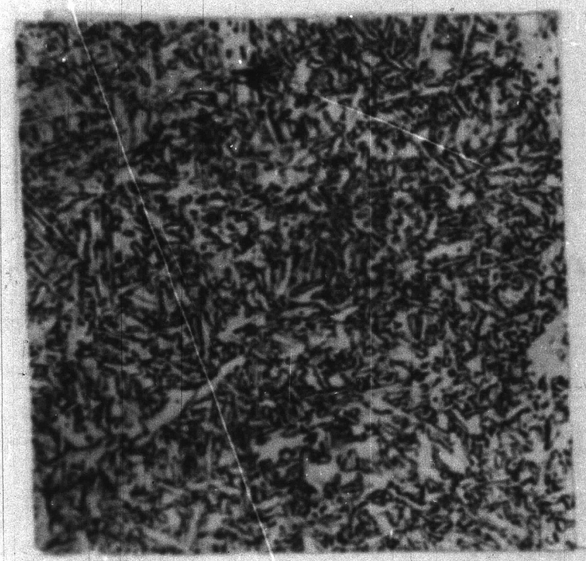

E 11018 Weld-metal VPN 287
1000 X Nital-Picral

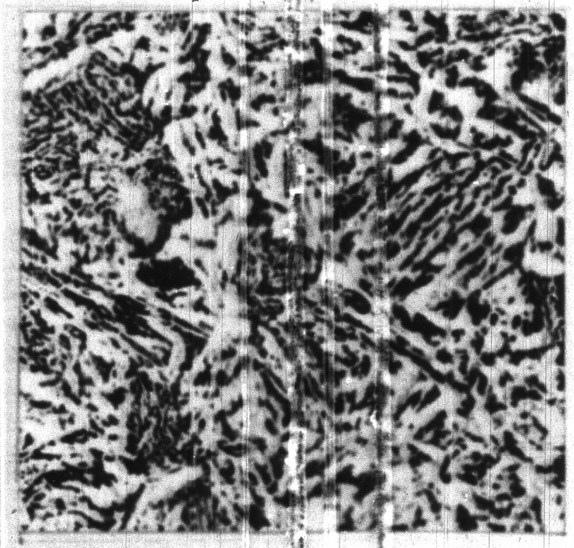

AISI 4140, As Rolled, VPN 292
1000 X Nital-Picral

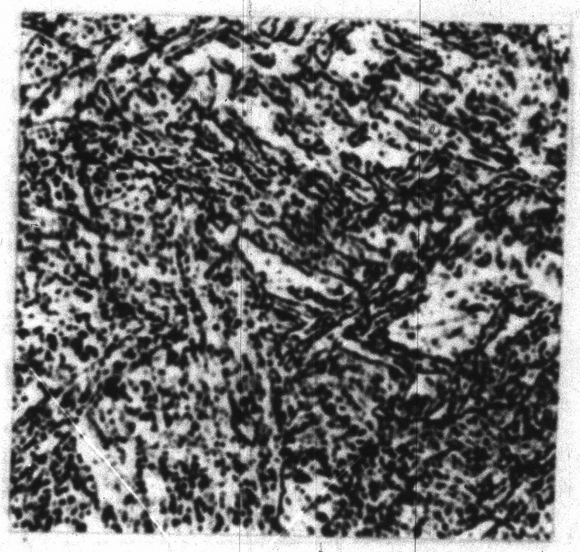

HY-80, Q-1610°F, T-1200°F
1000 X, Nital-Picral, VPN 221

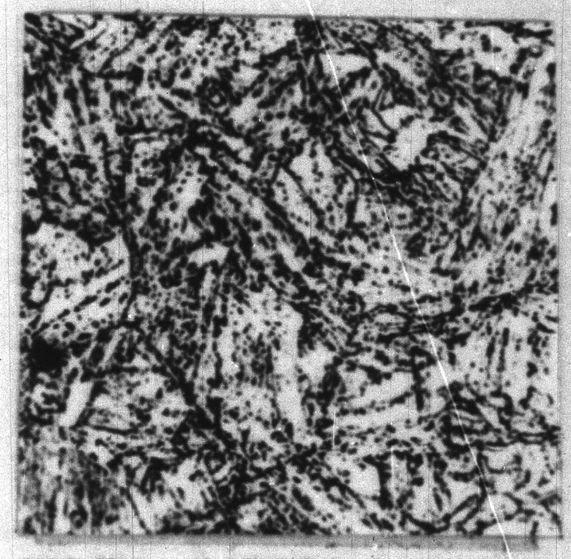

USS T-1, Q-1700°F, T-1200°F
1000 X, Nital-Picral VPN 297

Figure 3a. Photomicrographs of A212.

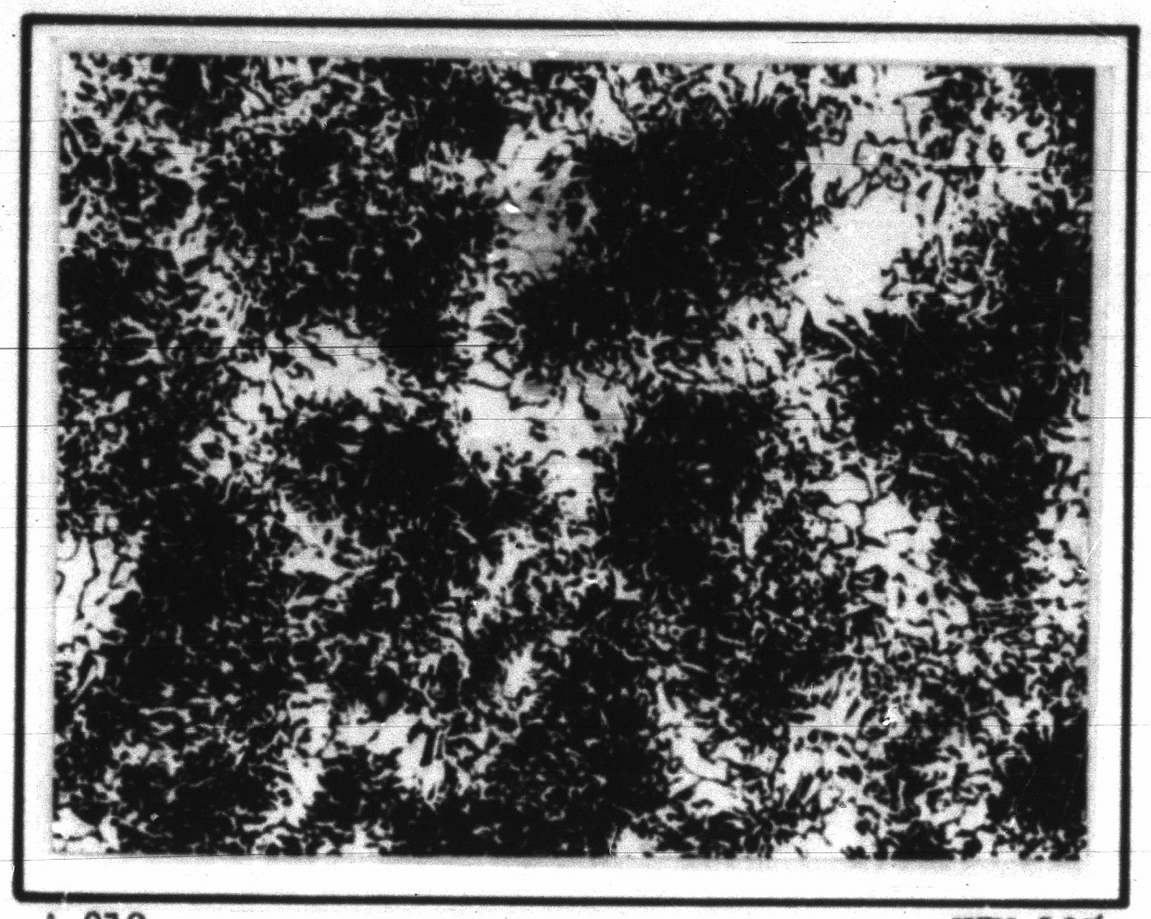

A-212 VPN 195
250 X, Nital-Picral
Peak temperature of 1635°F, cooling rate at 1300°F of 168°F/sec. Highly refined pearlite and ferrite.

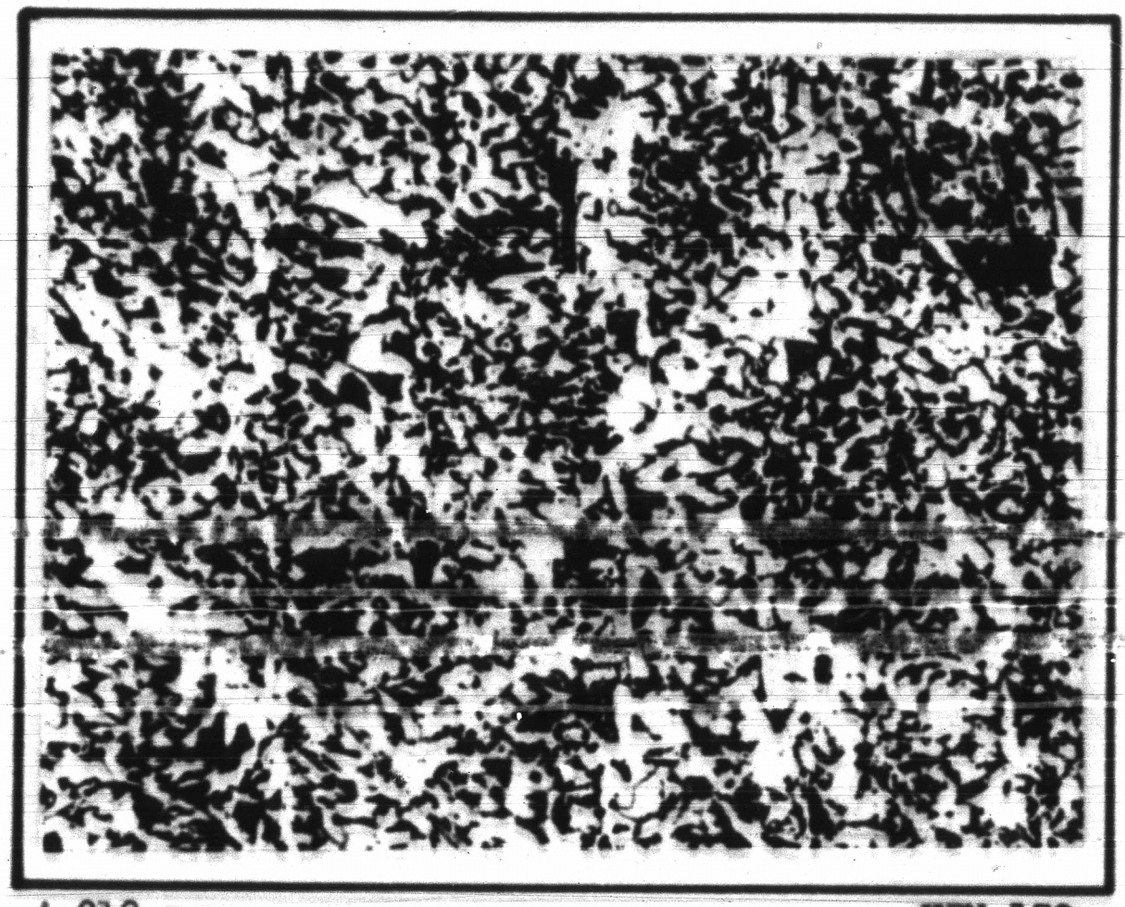

A-212 VPN 179
250 X, Nital-Picral
Peak temperature of 1610°F, cooling rate at 1300°F of 34.7°F/sec. Pearlite and ferrite.

Figure 3b. Photomicrographs of A212.

A-212 VPN 258
250 X, Nital-Picral
Peak temperature of 2390°F, cooling rate at 1300°F of 131.3°F/sec. Highly refined pearlite and acicular ferrite, some martensite.

A-212 VPN 197
250 X, Nital-Picral
Peak temperature of 2425°F, cooling rate at 1300°F of 21.7°F/sec. Pearlite and acicular ferrite.

Figure 4. Photomicrographs of E11018 Weld Metal.

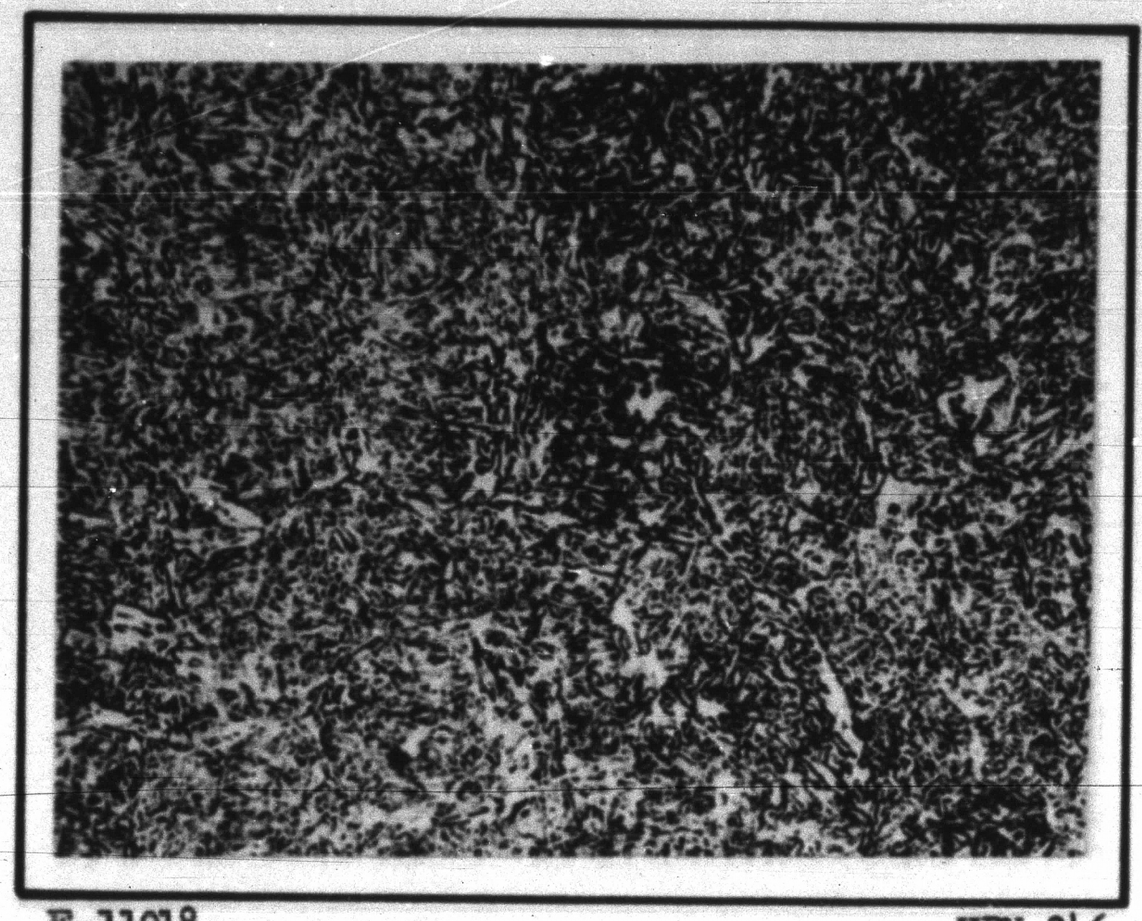

E 11018 VPN 246
250 X, Nital-Picral
Peak temperature of 2385°F, cooling rate at 1300°F of 25.3°F/sec. Ferrite and bainite.

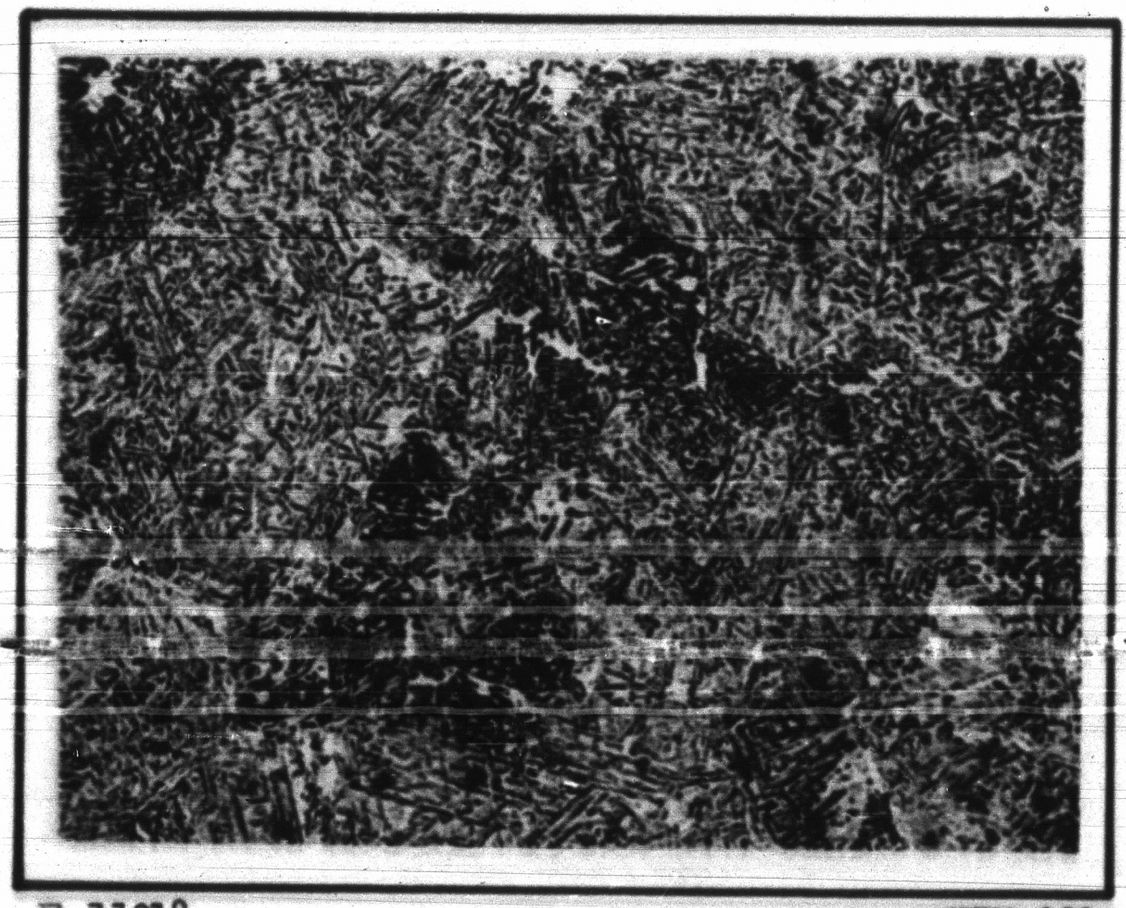

E 11018 VPN 322
250 X, Nital-Picral
Peak temperature of 2370°F, cooling rate at 1300°F of 136.7°F/sec. Bainite with some ferrite.

Figure 5. Photomicrographs of A302.

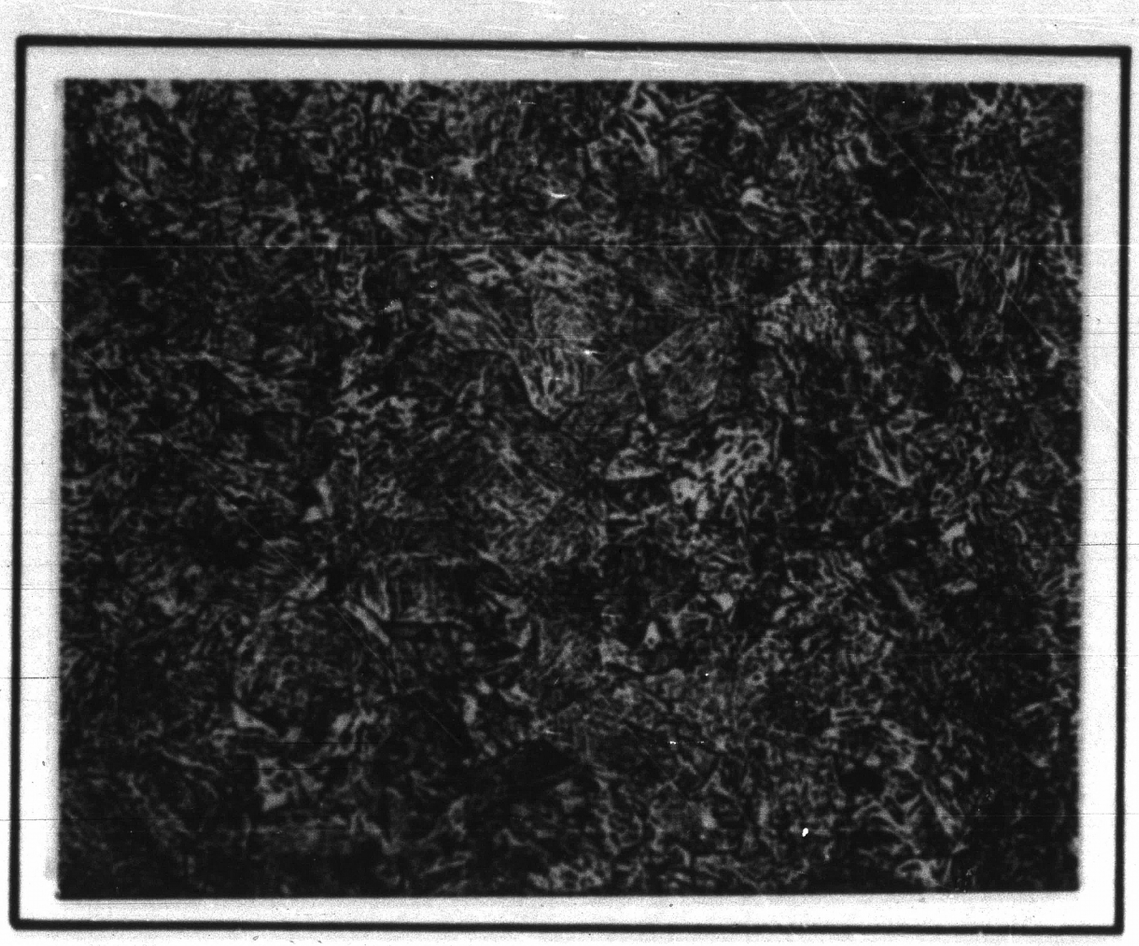

A-302 VPN 271
250 X, Nital-Picral
Peak temperature of 2080°F, cooling rate at 1300°F of 24.3°F/sec. Bainite.

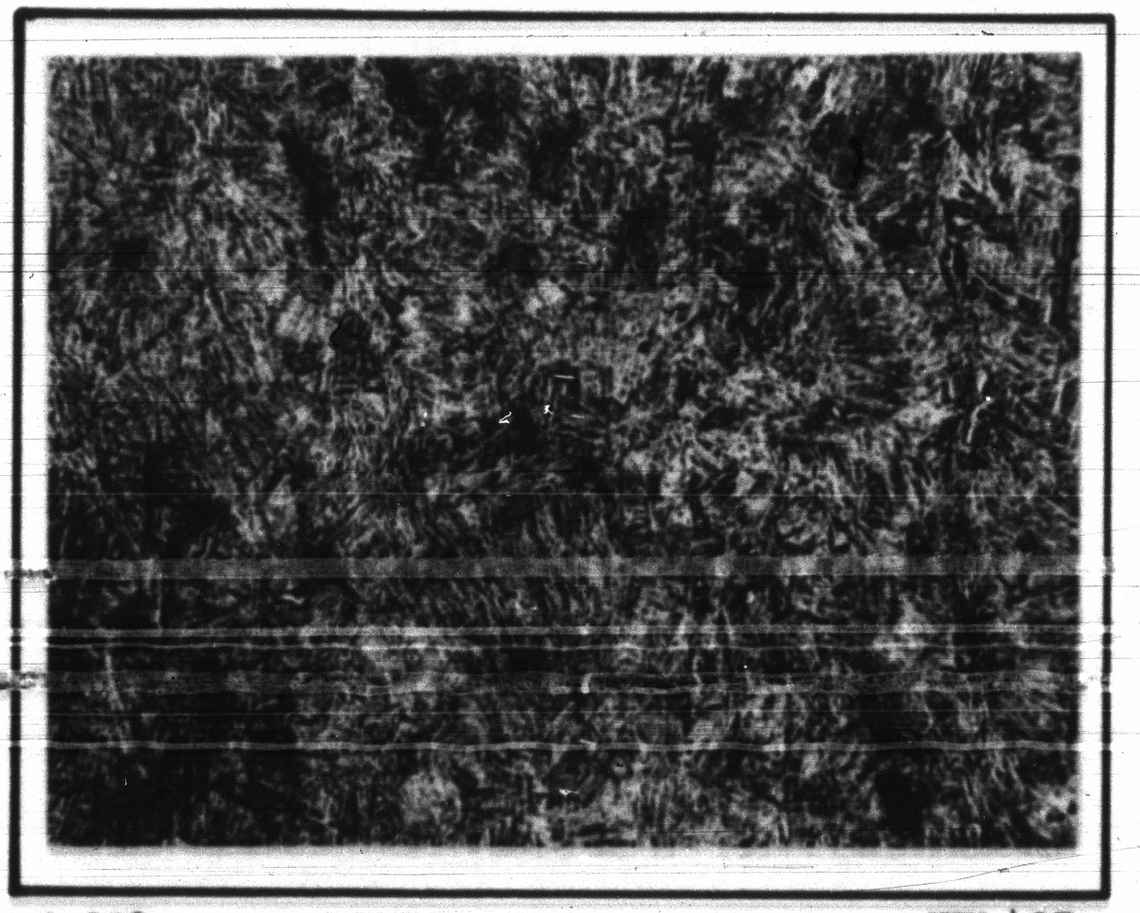

A-302 VPN 437
250 X, Nital-Picral
Peak temperature of 2035°F, cooling rate at 1300°F of 118°F/sec. Martensite.

Figure 6a. Dilatometric Curves of A212.

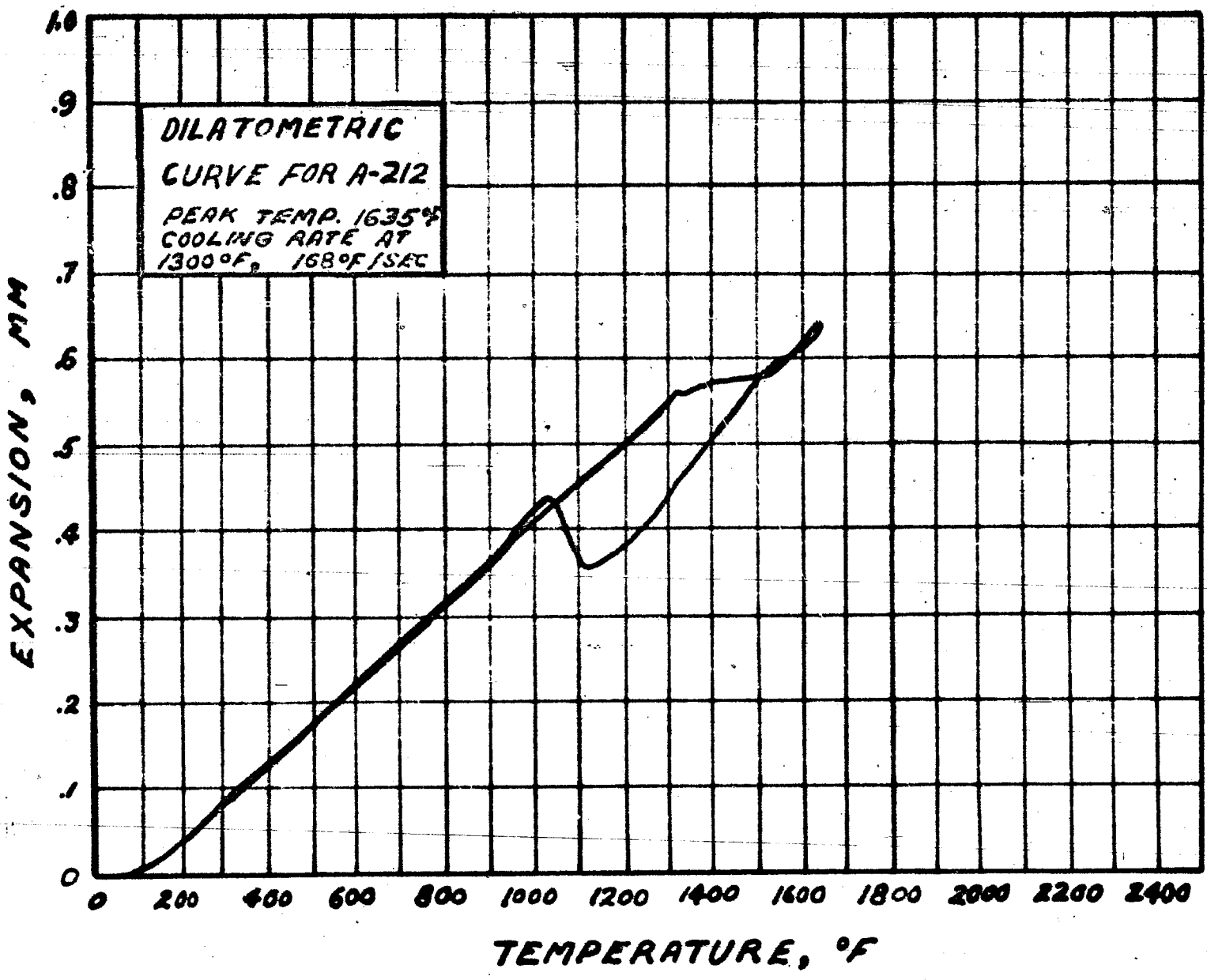
DILATOMETRIC
CURVE FOR A-212
PEAK TEMP. 1635°F
COOLING RATE AT
1300°F. 168°F/SEC
EXPANSION, MM
1.0
.9
.8
.7
.6
.5
.4
.3
.2
.1
0
0 200 400 600 800 1000 1200 1400 1600 1800 2000 2200 2400
TEMPERATURE, °F

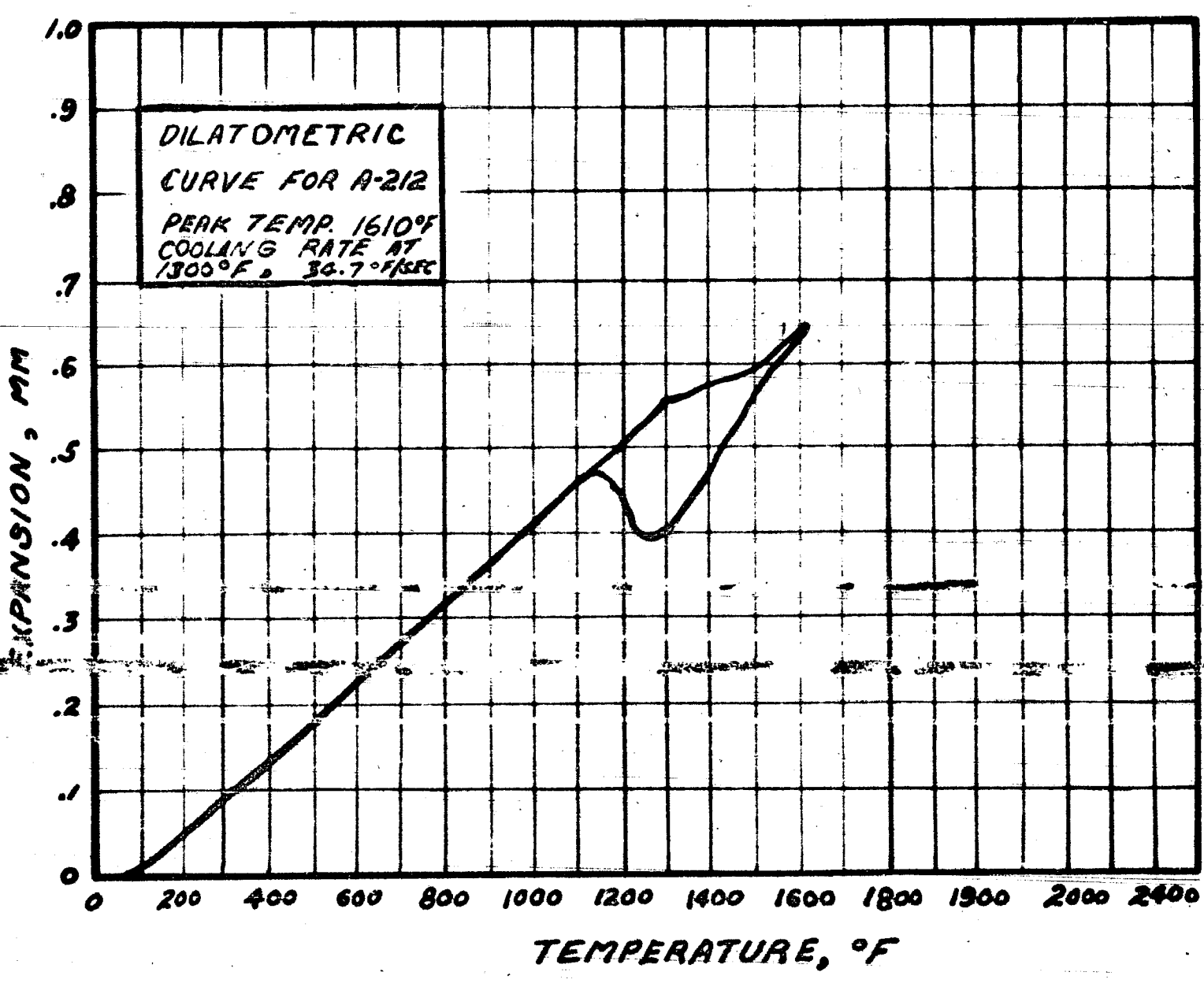
DILATOMETRIC
CURVE FOR A-212
PEAK TEMP. 1610°F
COOLANG RATE AT
1300°F. 34.7°F/SEC
EXPANSION, MM
1.0
.9
.8
.7
.6
.5
.4
.3
.2
.1
0
0 200 400 600 800 1000 1200 1400 1600 1800 1900 2000 2400
TEMPERATURE, °F

Figure 6b. Dilatometric Curves of A212.

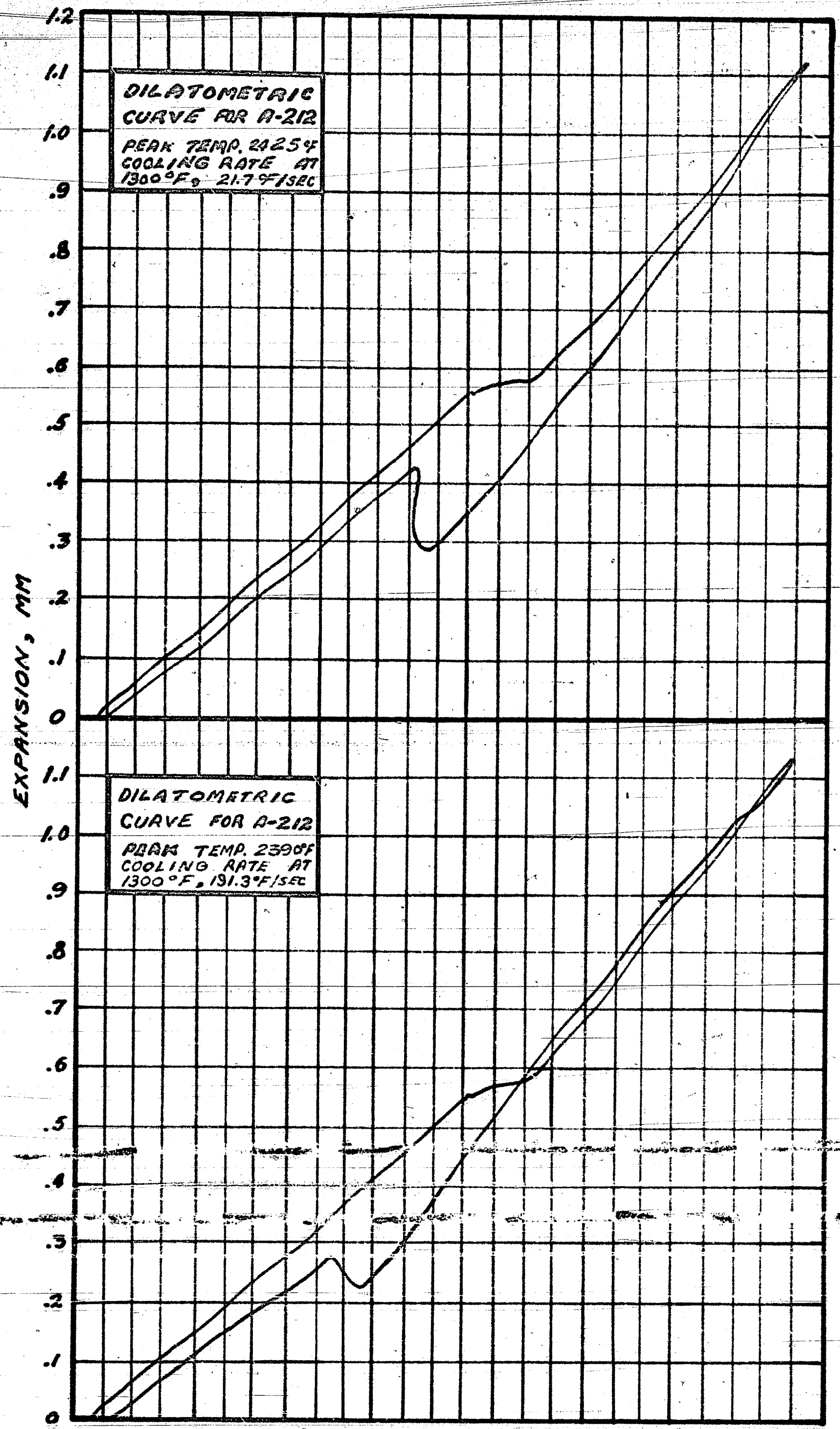
DILATOMETRIC CURVE FOR A-212
PEAK TEMP. 2425°F
COOLING RATE AT 1300°F, 21.7°F/SEC
DILATOMETRIC CURVE FOR A-212
PEAK TEMP. 2390°F
COOLING RATE AT 1300°F, 191.3°F/SEC
EXPANSION, MM
1.2
1.1
1.0
.9
.8
.7
.6
.5
.4
.3
.2
.1
0
200
400
600
800
1000
1200
1400
1600
1800
2000
2200
2400
TEMPERATURE, °F

Figure 7. Dilatometric Curves of E11018 Weld Metal.

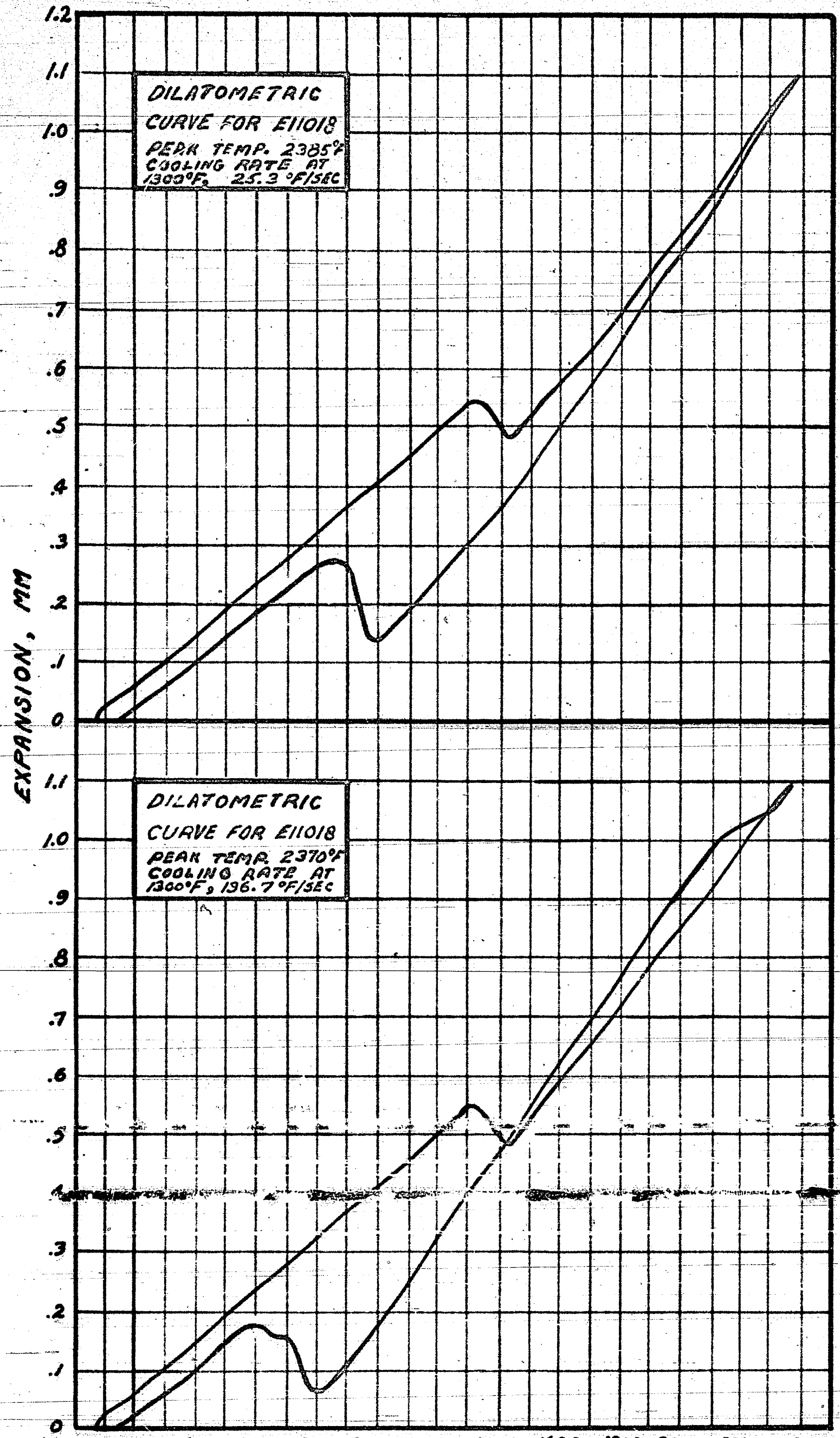
DILATOMETRIC
CURVE FOR E11018
PEAK TEMP. 2385°F
COOLING RATE AT
1300°F, 25.3 °F/SEC
DILATOMETRIC
CURVE FOR E11018
PEAK TEMP. 2370°F
COOLING RATE AT
1300°F, 196.7 °F/SEC
EXPANSION, MM
1.2
1.1
1.0
.9
.8
.7
.6
.5
.4
.3
.2
.1
0
200
400
600
800
1000
1200
1400
1600
1800
2000
2200
2400
TEMPERATURE, °F

Figure 8. Dilatometric Curves of A302.

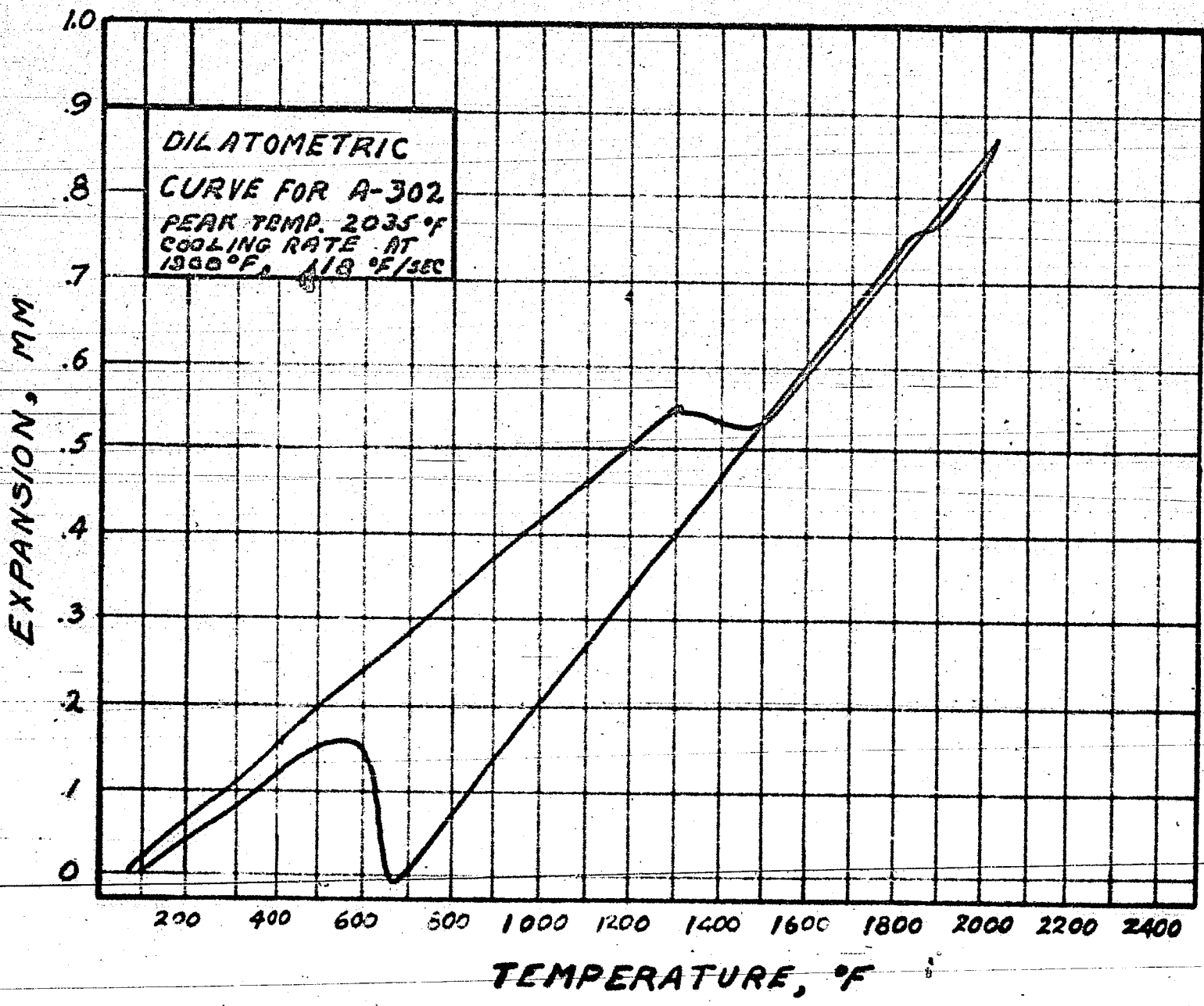
DILATOMETRIC
CURVE FOR A-302
PEAK TEMP. 2035°F
COOLING RATE AT
1900°F, 41.8 °F/SEC
EXPANSION, MM
1.0
.9
.8
.7
.6
.5
.4
.3
.2
.1
0
200
400
600
800
1000
1200
1400
1600
1800
2000
2200
2400
TEMPERATURE, °F

DILATOMETRIC
CURVE FOR A-302
PEAK TEMP. 2080°F
COOLING RATE AT
1300°F, 24.3 °F/SEC
EXPANSION, MM
1.0
.9
.8
.7
.6
.5
.4
.3
.2
.1
0
200
400
600
800
1000
1200
1400
1600
1800
2000
2200
2400
TEMPERATURE, °F

VITA

Lawrence Frank Bubba was born on April 2, 1929, in Easton, Pennsylvania. There he received his primary and secondary education, graduating from Easton Senior High School in June, 1946. In September, 1946, Lawrence entered Lafayette College and obtained a Bachelor of Science Degree in Metallurgical Engineering in June, 1950. In October, 1950, he entered the United States Air Force and was commissioned a second lieutenant in September, 1952. Lawrence was selected by the Air Force Institute of Technology as a candidate for a Master of Science Degree in Metallurgical Engineering, and he was subsequently sent to Lehigh University in July, 1958.

Presently he is serving as a Captain in the United States Air Force, assigned to the Air Research and Development Center, Wright-Patterson Air Force Base, Ohio.